

Study of pore pressure change during mining and its application on water inrush prevention: a numerical simulation case in Zhaogezhuang coalmine, China

Bin Zhu · Qiang Wu · Jianwen Yang ·
Tao Cui

Received: 22 May 2012 / Accepted: 21 June 2013 / Published online: 13 July 2013
© Springer-Verlag Berlin Heidelberg 2013

Abstract Most of water inrush incidents in coalmines are originally derived from a seepage flow through rock mass fractures, particularly in fault zones. Water inrush is typically caused by hydromechanical coupling interactions induced by human activities. Taking the Zhaogezhuang coalmine in northern China as an example, the progress of a lagging water inrush, which occurred at a depth of about $-1,100$ m, was simulated and analyzed based on the hydromechanical coupling mechanism. A 3D model incorporating the main structures of the study area was constructed based on the geological data and field investigation. The equivalent continuum medium was employed to describe fault zones. Processes of determining the mechanical, rheological and hydraulic parameters are discussed in details. Three hydromechanical coupling models

are applied: (1) the elastoplastic strain-fluid coupling mechanism in rock mass within the fault zone, (2) the inelastic creep-fluid coupling mechanism in rock materials within the fault gouge, and (3) the stress-permeability coupling mechanism in the fractured porous rocks. The evolution of water-recharge zones along the fault zone was presented in different mining phases. By comparing the simulated pore pressures with the in situ monitored ones, the following conclusions can be drawn: (1) the actual hydraulic behaviors are a combination of the long-term trends and short-term effects; (2) the creep-fluid coupling model reflects the rock hydraulic behaviors of long-term trends, while the elastoplastic strain-fluid coupling model demonstrates the short-term effects; (3) a prediction method called ‘time window’ for the risk of the lagging water inrush is proposed. Its feasibility is discussed.

Electronic supplementary material The online version of this article (doi:10.1007/s12665-013-2616-4) contains supplementary material, which is available to authorized users.

B. Zhu (✉)
Guangxi Scientific Experiment Center of Mining,
Metallurgy and Environment & Guangxi Key Laboratory
of Hidden Metallic Ore Deposits Exploration, Guilin University
of Technology, Guilin, Guangxi 541004, China
e-mail: zhubin1969@vip.sina.com; zhubin1969@qq.com

B. Zhu · J. Yang
Department of Earth and Environmental Sciences, University
of Windsor, Windsor, ON N9B 3P4, Canada

Q. Wu
State Key Laboratory of Coal Resources and Safe Mining,
China University of Mining and Technology,
Beijing 100083, China

T. Cui
CSIRO Land and Water, 41 Boggo Road,
Dutton Park 4102, Queensland, Australia

Keywords Pore pressure · Mining · Water inrush ·
Numerical simulation · Hydromechanical coupling

Introduction

Mining water inrush is a type of serious incident occurring in the form of groundwater intruding into an underground opening space, for example, drifts, openings or working faces. A specific water inrush is the lagging water inrush in which the water floods into an opening space from aquifers through fractures within fault zones. There is usually a time span from fault zones exposure to water inrush occurrence during the process of coal mining. It is a huge threat to the coalmines in China, and difficult to prevent (Wu et al. 2011a). The 272 coalmines of 624 unified distribution coalmines in China are threatened by water flooding. From 1955 to 2000, there were 1,500 cases of serious mining

water inrush incidents, almost 80 % of which were involved with the fractured fault zones and had the features of lagging water inrush (Coalfield Geological Central Bureau of China 2000). A typical lagging water inrush happened at the 9th level of No. 1 crosscut at a depth of approximately -730 m within the eastern mining area of Zhaogezhuang coalmine in 1972 (Wu et al. 2002; Zhu 2009).

The study focus of excavation-induced water inrush has evolved over the past decades. In the beginning, much interest was focused on the volume of water inflow assessment for rock tunnel (Goodman et al. 1965; McFeat-Smith et al. 1985, 1998; Heuer 1995). Later, more evidence showed that the excavation-induced changes in stress and deformation of rock masses result in permeability variations, and eventually lead to water inrush into an opening space where there exist weak tectonic structures (e.g., faults, joints, fractures) connecting with aquifers. The issue has been studied in laboratories and fields by many scholars for the original goal of safety of nuclear waste repositories (Börgesson et al. 1992; Olsson 1992; Emsley et al. 1997; Sugihara et al. 1999; Bäckblom and Martin 1999). One of the most highlights is the field test to the permeability change in the excavation disturbed zone (EDZ) around tunnels in Sweden as an important part of the Stripa project (Witherspoon 2000).

The occurrence and development of mining lagging water inrush is a representative process of hydromechanical (HM) coupling, implying the physical interaction between hydraulic and mechanical processes. HM interaction is common in geological media (e.g., soils and rocks) because such media contain pores and fractures that can be fluid filled and deformable. In general, a fluid-saturated porous or fractured rock mass can deform as a result changes of the external load and/or the internal pore-fluid pressure (Rutqvist and Stephansson 2003). It is reasonable that the processes of mining lagging water inrush can be investigated by considering the coupling between fluids and deformation.

For various reasons, unfortunately, the deliberately designed in situ experiments to study the mining lagging water inrush and its HM coupling process are almost impossible (Gray 1993), and specialized physical prototype tests are difficult to simulate the complex underground environment. Thus, numerical simulation based on field observations has become a reasonable choice for studying some water inflow events, particular the small lagging water inrush events occurring during the course of mining.

In this research, a small-scale mining lagging water inrush that occurred in the 13th level no. 1 crosscut, at a depth of about $-1,100$ m, in the eastern part of Zhaogezhuang coalmine, is described. A robust numerical model was built using FLAC^{3D} according to the recorded

Fig. 1 a Main tectonostratigraphic subdivisions of Kailuan coalfield affiliated with Kuailuan group corporation, and outcrops of coal measures hosted in Carboniferous–Permian (C–P) strata; **b** Simplified geological map of Zhaogezhuang coalmine showing the locations of the underground drifts extension. Alluvial-eluvial deposits prevail except where C–P and C–O outcrops occur. P—Permian sand-shale; C—Carboniferous sandstone; O—Ordovician limestones; C—Cambrian limestones; Z/Sinian sandstone (Wang et al. 1977); **c** A–A' profile of Zhaogezhuang coalmine

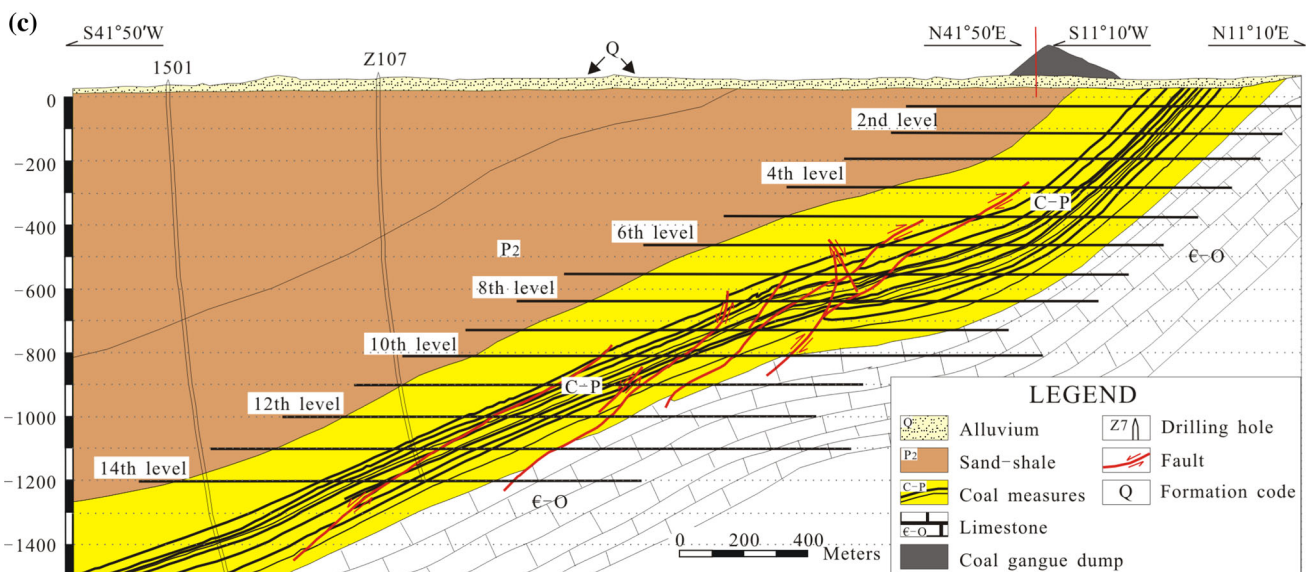
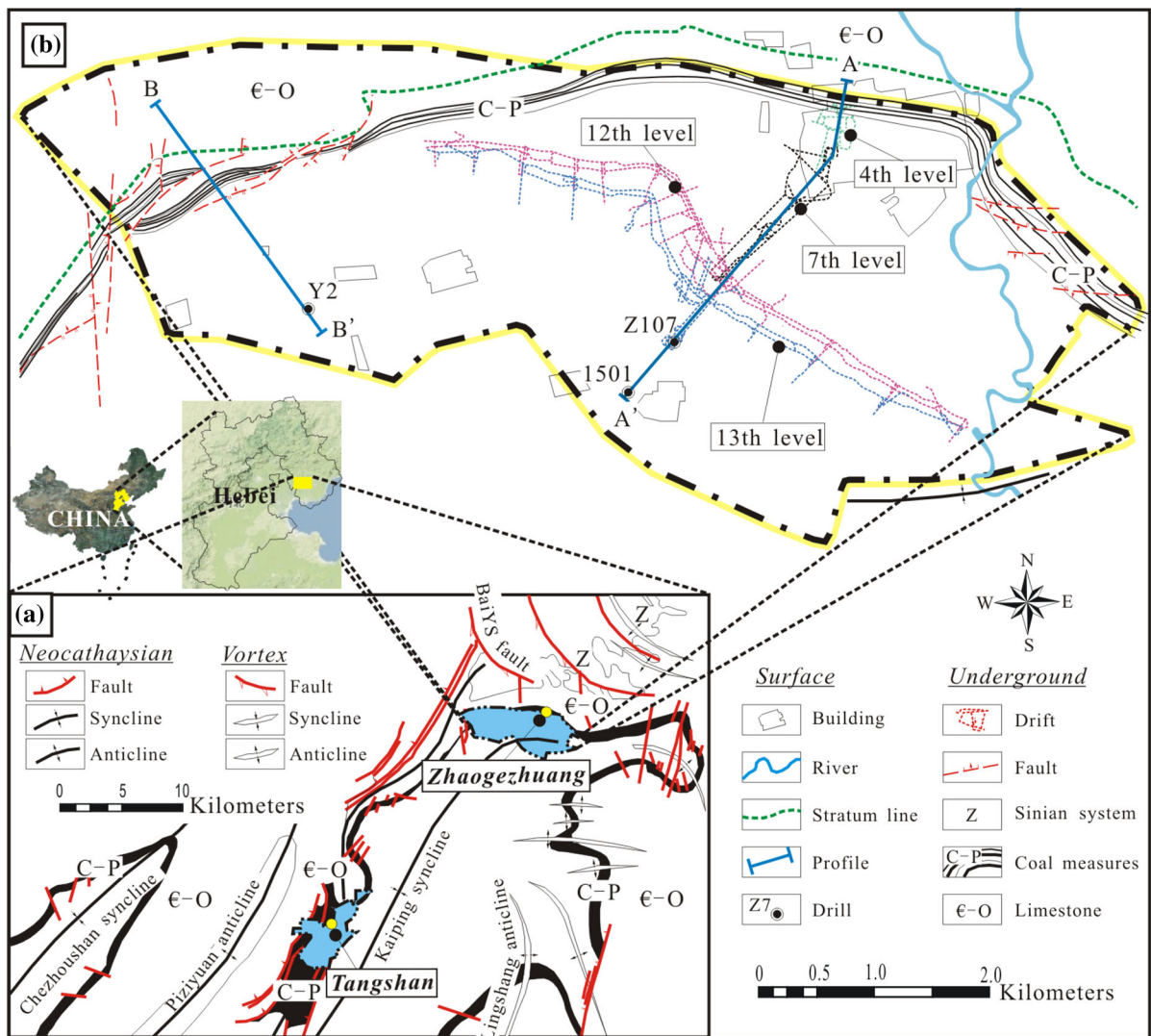
event process and geological setting. Three HM coupled methods, consisting of direct and indirect HM coupling (Rutqvist and Stephansson 2003), are applied: (1) the elastoplastic strain-fluid coupling, a direct HM method of considering the fractured porous rocks as elastoplastic materials, (2) the inelastic creep-fluid coupling, also a direct HM coupling method of considering rock mass as viscoelastic materials, and (3) the stress-permeability coupling in fractured porous rocks, an indirect HM coupling method regarding the influence of stress-induced permeability variations during mining.

Background of geologic conditions and study site

Geological setting

Zhaogezhuang coalmine is located within the northeastern suburb, an area named “Guye region”, of Tangshan city, Hebei province, north China (Fig. 1), covering an area of approximately 40 km². It has a semiarid climate and warm temperate with clearly cut seasons. Mean annual precipitation is about 614.7 mm. The surface covering is mainly composed of alluvial-eluvial deposits with a depth of 0 – 40 m. As a result of the Neocathaysian structural system, a series of compression-shear folds and faults in NNE direction occur alternately, representing the main tectonic features of this area. Due to the influence of the local vortex structure, in the east wing of Kaiping syncline (the coalmine-hosting area of Kaiping coalfield), a few extensional folds and faults are emerging (Fig. 1a). To the north edge of Zhaogezhuang coalmine area, the stretch of up and down mountains is the outcrop of Cambrian–Ordovician (C–O) limestone, with an elevation of 100.0 – 290.0 m. They are just the outcrops of the Kaiping syncline, a wing extended and exposed out of the ground surface (Fig. 1b).

Zhaogezhuang coalmine is situated just at the Kaiping syncline's tip (Fig. 1a), the end of a syncline axis characterized by a dramatic turn from around $N34^{\circ}E$ to almost E–W direction due to a strong squeezing and twisting tectonic force (Wang et al. 1977). The coal measures are hosted in the Carboniferous–Permian (C–P) stratum distributing on the plane, as shown in Fig. 1. On the profile, they have a very asymmetrical shape, with a 30 – 40° dip in



the eastern wing and an approximately vertical or even overturned dip in the western wing, respectively. As the oldest Chinese coalmine enterprise with more than 100 years of mining history, the Kailuan group corporation has constructed a complicated underground spatial structure, in which 14 mining levels (Fig. 1c) consist of a drift-digging length of up to 200 km. The 4th, 7th, 12th and 13th levels of drifts are illustrated using dashed lines with different colors in Fig. 1b. Until now, the maximum depth of coalmining has reached $-1,200$ m (the 14th level; Fig. 1c).

In this coalmine, the main aquifer potentially flooding to the mine is dominated by the Majiagou limestone group that is composed of thickly bedded and pale grey shelf limestone with a thickness of about 400 m. The aquifer is hosted within the upper Ordovician sequence and called the Ordovician limestone aquifer. As shown in Fig. 1c, this aquifer is inclined and can get rainfall recharge from its outcrop. Also, with the features of the synclinal structure and the developed fractures, this aquifer is a good storage and transport channel for groundwater. Within the current range of mining at about 1,200 m depth, the potentiometric pressures could reach 8.0–9.0 Mpa. In addition, some subordinate aquifers in the Carboniferous–Permian stratum, which are fractured and composed of medium-coarse sandstone, occasionally become main water pathways to threaten the mining activities. Particularly, the aquifer located between the thin-layer of limestone called K_6 and the 12th coal seam floor, which is about 13–18 m in thickness and named the coal measures aquifer, is remarkable because of its potentially hydraulic connections with the Ordovician limestone aquifer through the fractured fault zones. It is possible that there is a certain hydraulic link among these aquifers, in particular, when water conductive faults pass through them (Wang et al. 1977), as described in the following case study.

Study site

The study site is at the depth of $-1,100$ m near the 13th level of no. 1 crosscut in the eastern Zhaogezhuang coalmine. A 3-D model incorporating the main geological features and the mining structures of Zhaogezhuang coalmine has been constructed using ArcGIS (Fig. 2). As mentioned above, a small lagging water inrush incident occurred in the 13th level of no. 1 crosscut (Fig. 2b) when the 12th-upper coal seam was mined in 2003. At the beginning, only a few slow water-sprays were observed from drift walls nearby the no. 1 crosscut; thus people did not pay enough attention. However, when the 12th-lower coal seam was mined in an area called the 3132_1 face from May 2004 to July 2005, water-spraying became worse gradually, with a water inrush range expansion from 60 to 150 m along the drift wall (Fig. 2b). During the mining process, a water discharge of 1.1–1.6 m^3/min and a water

pressure of 4.9 Mpa were recorded and the roadway floor was heaved up to 162 mm. The normal mining was forced to be suspended from August 19 to September 5, 2005. After the mining was resumed, three working faces of the 3132 (3132_1, 3132_2 and 3132_3) were mined until March 2006. The water inrush discharge remained in the range of 0.5–1.0 m^3/min with a water pressure of 0.4–2.9 Mpa. After that, the water inrush shows a stable and slow decline.

By initial analysis, the water inrush was related to a branch of the VIIIth fault that connects the C–O limestone aquifer with the coal measures hosted in a C–P stratum. However, the discharge or the strength of this water inrush was not the same as the serious flooding, with a water discharge up to 52.71 m^3/min incident, that occurred at the 9th level of no. 1 crosscut in 1972 (Zhu 2009). It seems that there exist other water sources and pathways. In order to determine how the water inrush occurred, two slant boreholes (Monit.1 and Monit.2), were drilled with different orientations from the 13th level drifts (Fig. 2b) to serve as in situ monitoring points. The water pressures of the slant boreholes were measured from August 12, 2005 to August 7, 2007. The scatter plots of the water discharge and the water pressure versus the corresponding dates are illustrated (Fig. 2c) (the water discharge at Monit.2 was not recorded). There are some short-term fluctuations in both the water discharge and the pressure evolutions (Fig. 2c); however, slow and gradual depletion trends are obvious over the whole monitoring period.

Numerical model

Figure 3 shows a schematic representation of the geometry, main structures and boundary conditions of the study site, with a dimension of $320 \times 200 \times 230$ m in x , y , z direction and a depth ranging from $-1,000$ to $-1,230$ m. The mechanical boundary conditions are a uniformly applied stress, σ_z , equal to 23 Mpa of dead weight over the upper boundary, and a fixed movement on the lower and the lateral boundaries. The numerical model was built for a large-scale hydrogeological unit which includes the Ordovician aquifer boundaries of the whole coalmine. Based on a long-term monitoring of the piezometric levels and the amount of dewatering from the aquifer during mining, the piezometric levels fluctuated in the range of -200 to -250 m from 1991 to 1999 and the aquifer is spatially recharged from the natural hydrogeological boundaries with a total flux of 0.483–0.533 m^3/s inflow due to the permeable bare Karst region widely distributed in the outside of north coalmine border (Cao and Qi 2004).

As shown in Fig. 3b, the hydraulic boundaries of the numerical model were described by the mixed-III kind boundary conditions in which there was a combination of the specified-head boundary and the specified-flux

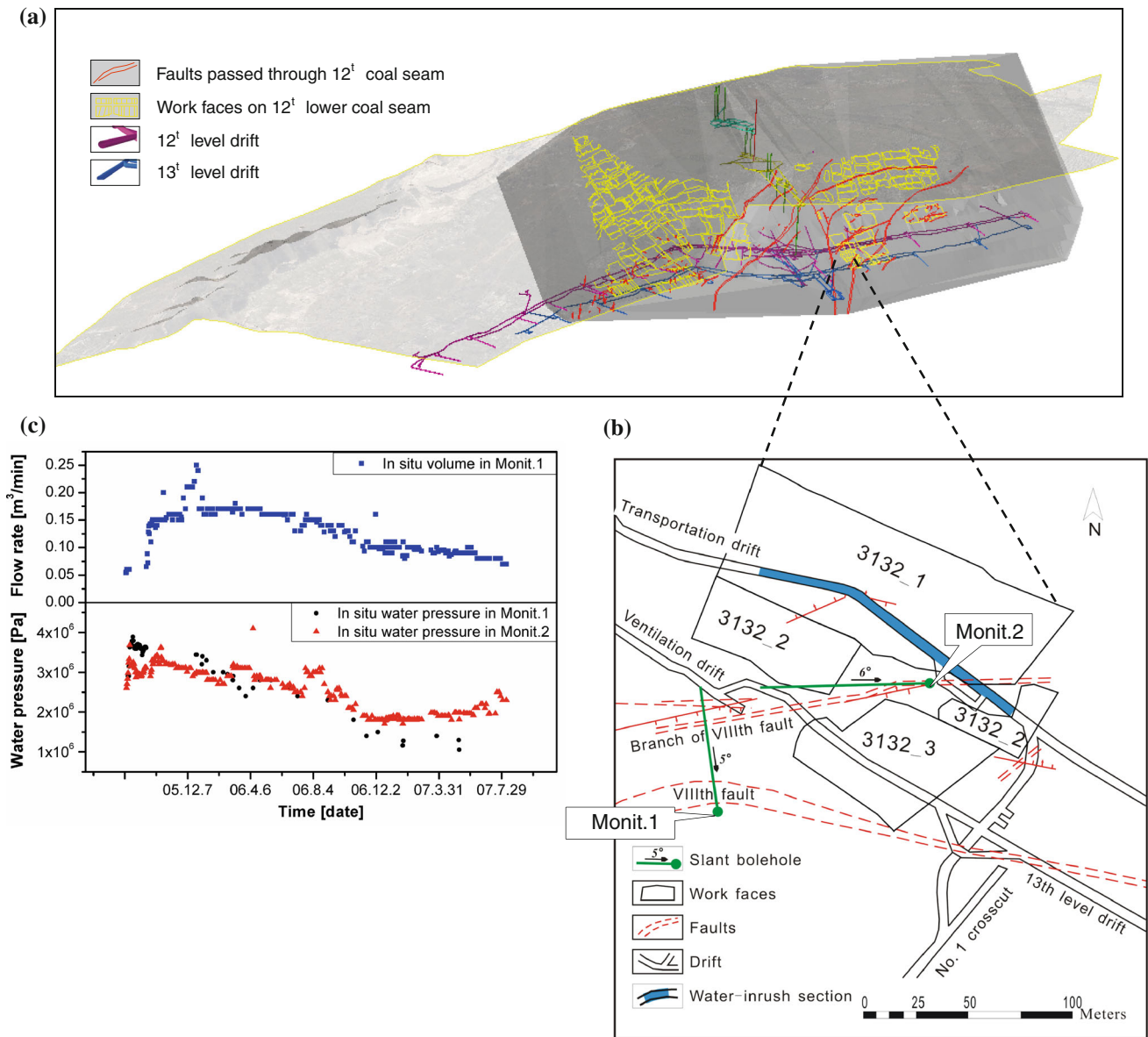


Fig. 2 **a** 3D perspective view of the study area illustrating some information such as faults, coal seams, drifts and working faces in the study area; **b** top view of a section of the transportation drift in which water inrush occurred. The working faces and faults that lie above the

13th level drift are also shown; **c** In situ observation data of flow rate and water pressure in Monit.1 and Monit.2 in no.1 crosscut of the 13th level in the water inrush field

boundary. Corresponding to the specified-head boundary in the depth of 1,100 m, the water pressure of 8.8 Mpa was applied in the Ordovician aquifer. In the Carboniferous coal measure's aquifer, the water pressure of 4.5 Mpa, which mainly come from the Ordovician aquifer with a loss of head, also was preset. Two areas were assigned to the specified-flux boundary. One area is the natural north hydrogeological boundary of approximately 151.3 km² with a total flux of about 0.5 m³/s; the other area is the lateral boundary of approximately 0.023 km²

(200 × 115 m) of the numerical model in which a flux of 7.6×10^{-5} m³/s inflow was calculated.

As shown in Fig. 3b, c the sketch of model mesh consists of seven types of rock materials, which are the Carboniferous fine sandstone, the 12th-lower coal seam, the medium-coarse sandstone, the fault gouge, the mylonite rock, the sandstone and the Ordovician limestone. Each type of rock was represented, by a group of blocks in FLAC^{3D} software (Itasca Consulting Group 1997; Granet et al. 2001; Caillabet et al. 2000). The red cells represent

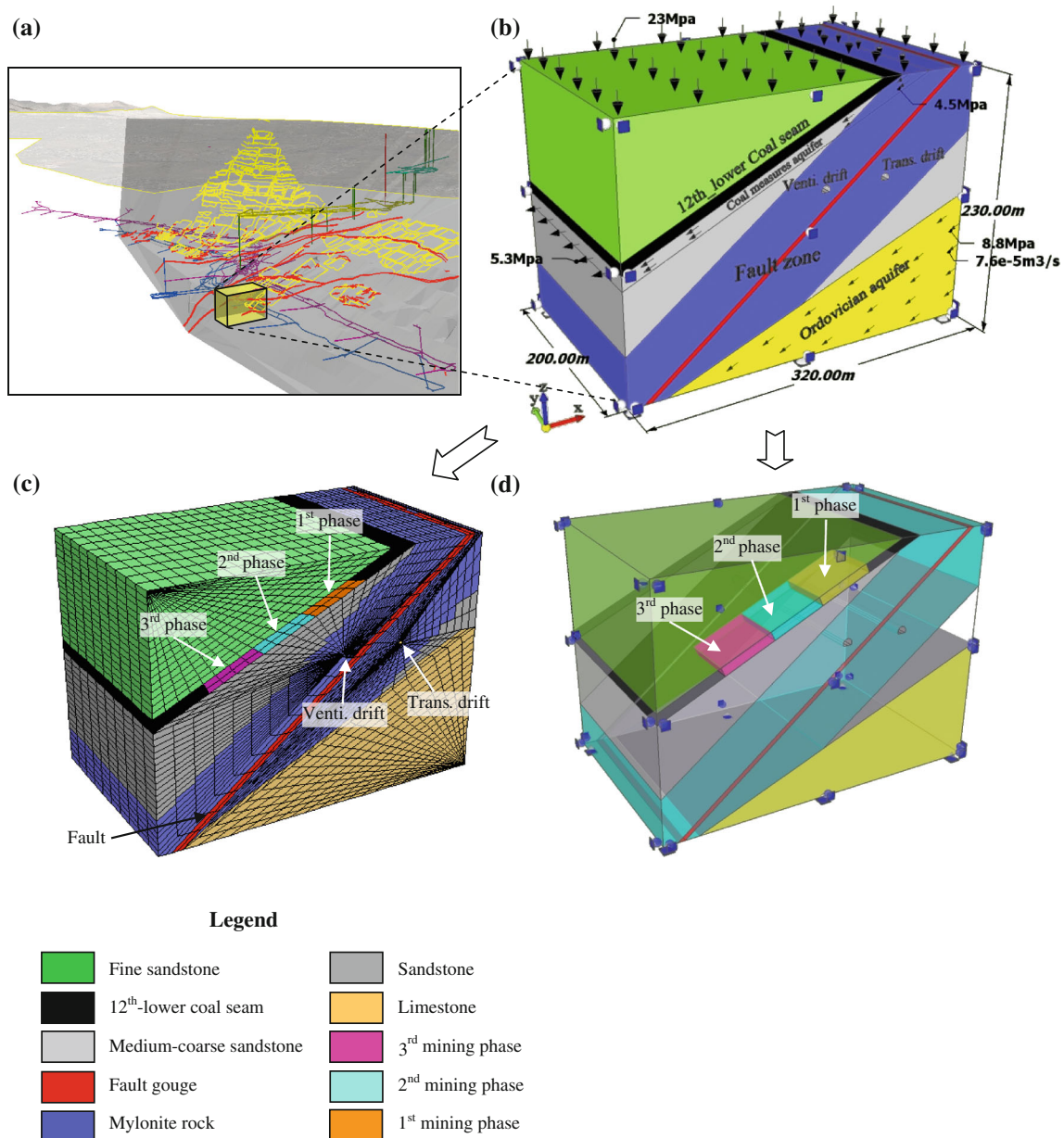


Fig. 3 3D diagrams demonstrating the process of numerical model construction. **a** Spatial location of the model. **b** Conceptual model and definition of boundaries used in the numerical simulation. **c** Grid model for tectonic structure, deposits, mining phases and drifts. **d**


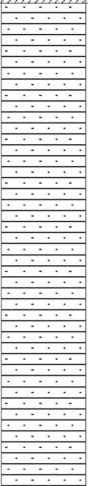

















X-ray transparent diagram showing the model. Notice that every mining phase is composed of $50 \times 50 \times 4.2$ m coal seams for simulating the process of coal excavation

the fault gouge, a soft-rheology-plastic material in the VIIIth fault. Fault movements can affect the surrounding rocks and cause them to be metamorphous and fractured. Previous studies have verified that the process also happened in the vicinity of the VIIIth fault (Wu et al. 2002). The blue cells surrounding the VIIIth fault, represents the mylonite, which is a by-product of squeezing, shearing and tortuosity in rock fractures. According to the boreholes' data (Table 1), the VIIIth fault zone, including its branch, is about 80 m in thickness.

Parameter determination

The determination of mechanical and hydraulic parameters of rock masses is always referred to be a problem of scale dependency; and consequently how to use equivalent continuum media with realistic parameters to describe the macroscopic behavior of fractured and porous rocks becomes very complicated (Long et al. 1982; Sitharam et al. 2001). Comparing the model size ($320 \times 230 \times 200$ m) with the opening spaces (3–5 m

Table 1 Typical geological column of boreholes overlying the Ordovician limestone in Zhaogezhuang coalmine

System	Formation	Thickness/m		Interval of key bed/m	Column	Description of rock	Features zoning
		Accumulation	Seam				
Permian	Tangjiazhuang		7.72	7.72		Bauxitic layer: grey, fine and glossy	Coal measures: a zone main mining seam hosted in study area
				163.23		Sandstone: grey or dark grey, medium-coarse sandstones interbedded with siltstone, fine stone or thin claystone	
		170.95				3rd coal seam: black, thin layer in 30–90 cm	
		210.00		16.25		4th coal seam: black, thin layer in 30–90 cm	
						Sandstone: grey or dark grey, siltstone	
	Damiaozhuang		0.83			5th coal seam: black, thin layer in 60–90 cm	
			1.43–6.13 Ave: 4.30	148.80		7th coal seam: black, main mining seam	
						8th coal seam: black, main mining seam	
		281.00				9th coal seam: black, main mining seam	
						11th coal seam: black, main mining seam	
Carboniferous	Zhaogezhuang					12th-upper coal seam: black, main mining seam	
						12th-lower coal seam: black, main mining seam	
						K6 limestone: dark grey, thin layer in 1–2 m	Confined aquifer
		401.00		76.88		Sandstone: grey or dark grey, mainly with siltstone, fine stone or claystone	
						K4 limestone: dark grey, thin layer in 1–2 m	
	Kaiping					K3 limestone: grey, thin layer in 2–3 m	Fault zone: fractured, filled with gouge and surrounded by mylonite rock
			2.50–3.00 Ave: 2.77	45.12		Sandstone: grey or dark grey, mainly with siltstone, fine stone	
		458.00				Bauxitic claystone: grey	
	Ordovician	Majiagou	>600.00	>600.00		Limestone: grey, fractured	Confined aquifer

diameter of engineering-scale drifts), the ratio of scale is great enough to diminish the scale effects based on the principles of continuum mechanics.

Mechanical parameters

The numerical model input parameters, such as the in situ stress field, the rock strength, and deformation modulus, are never known precisely. There are always uncertainties in these parameters; some of the uncertainties are intrinsic and the others arise from the lack of knowledge or understanding (Cai 2011). Perello (2011) presented a systematical analysis to various types of geological uncertainties.

The mechanical parameters, such as E_i uniaxial compression modulus, c_i , ϕ_i Morh-Coulomb parameters, σ_{ti} tensile strength, can be obtained in a laboratory and in situ test in association with previous research results (Zhou et al. 2000; Wu et al. 2004). Justo et al. (2010) provided a method to estimate the modulus and strength of fractured rocks based on different rock mass classification systems, which include the Q system (Barton et al. 1977), the rock mass rating (RMR) system (Bieniawski 1984), the geological strength index (GSI) system (Hoek and Brown 1997), and the parameter values obtained in laboratory and in situ tests. It is a valuable way to obtain the mechanical parameters of rock masses through which geological uncertainties are reduced as much as possible; however, it is time-consuming and costly. In this study, the RMR system was adopted in association with previous engineering experiences. The mechanical parameters used in our numerical simulation are shown in Table 2.

Rheological parameters

As mentioned above, the VIIIth fault zone is viewed as a weak zone, which is fulfilled with soft-rheology-plastic fault gouge, i.e. the black fault mud or grey-black mylonite. Zhou et al. (1998, 2000) collected in situ samples from the fault zones of the Zhaogezhuang coalmine and conducted

triaxial and uniaxial rheological tests. Tao et al. (2005) evaluated the fitting effects using two types of visco-elastoplastic creep models, i.e., the Burgers creep model and the Nishihara creep model, and conclude that the latter was more suitable than the former to depict the grey-black mylonite present in the study area.

In addition, some empirical models are more flexible and convenient to describe the rocks of creep properties. The power law creep models, also called the Norton power law creep models (Norton 1929), are commonly used (Gerya et al. 2002; Sun 2007):

$$\dot{\epsilon}_{cr} = A \bar{\sigma}^n t^m \quad (1)$$

$$\bar{\sigma} = \left(\frac{3}{2}\right)^{1/2} \left(\sigma_{ij}^d \sigma_{ij}^d\right)^{1/2} \quad (2)$$

where $\dot{\epsilon}_{cr}$ is the creep rate, A , n and m are the rheological parameters obtained by fitting results of rheological test, $\bar{\sigma}$ is the equivalent stress, and σ_{ij}^d is the deviatoric part of σ_{ij} .

Based on the results of creep test by Zhou et al. (2000), a few works of re-fitting these data using the power law have been done in order to determine our rheological parameters. A strong fluctuation in the parameters was found. Parameter A varies from 10^{-4} to 10^{-8} in four orders of magnitude, and parameter n and m also having a great variation. These results mean that the rock materials making up of the fault gouge have a great variation in the rheology mechanical behavior in a sample scale.

In order to acquire equivalent rheological parameters for the numerical simulation in model scale, a comprehensive method of combining the data of in situ tests and in-door rheological analyses is worth considering. At the depth of $-1,000$ m, according to the stress testing results using stress relaxation method, the in situ ground stress usually reaches 20–25 Mpa, occasionally up to around 30 Mpa, such as in the stress concentration areas. However, due to the limitation of instruments, only a few triaxial creep testers are able to reach a very high confining pressure and completely resume the scenes of in situ stress environment; and hence an in situ creep test should be the best way to acquire the equivalent rheological parameters.

Table 2 Mechanical parameters of rock masses obtained using the RMR system in association with previous engineering experiences

Stratum	Compression parameters		Morh-Coulomb parameters		Tensile strength σ_{ti} (Mpa)	Density ρ_i (kg/m ³)
	E_i (Gpa)	μ_i	c_i (Mpa)	ϕ_i (°)		
Fine sandstone	19.0	0.24	2.000	42	3.0	2,600
12th-lower coal seam	0.2	0.40	0.070	27	0.5	1,500
Medium-coarse sandstone	20.0	0.25	2.200	24	1.3	2,650
Fault gouge	0.6	0.45	0.300	23	0.1	2,600
Mylonite rock	0.2	0.25	0.013	18	1.0	2,000
Sandstone	23.0	0.23	5.000	44	4.0	2,800
Limestone	25.0	0.22	8.000	45	6.0	2,700

Wu and Chen (1992) employed the in situ creep test method to study the rheological behaviors of metamorphic rocks in the Jinchuan copper mine, Gansu province, China. Chen et al. (2009a, 2009b) studied the rheological properties of mudstone in the Xinji coalmine, China, using both the in situ and in-door creep test methods, and acquired the rock’s rheological parameters by fitting the in situ and in-door test data to the power law creep model. Some parameters and formulas of the power law creep models acquired in China are shown in Table 3.

Based on the review mentioned above, A is between 10^{-8} and 10^{-4} ; n and m are from 1.2 to 5.39 and $-0.985-0.25$, respectively. Firstly, the listed results of the creep tests can give a rough idea of various parameters. They can be obtained from a trivial work such as a non-linear surface fitting and can be done efficiently by the Gauss2D fitting function when the exponential function of the power law creep model is transformed into the logarithmic function. Secondly, in consideration of the parameters variability, it is necessary to add and refer to some other engineering experiences; for example, those listed above in Table 3, in case large errors occur. Thirdly, a large number of trial works would also be helpful to optimizing these parameters. After all, the compromise power law creep model for this simulation is finally determined explicitly as follows:

$$\dot{\varepsilon}_{cr} = 1.01 \times 10^{-7} \bar{\sigma}^{3.0} t^{0.1} \tag{3}$$

Hydraulic parameters

Rocks permeabilities have been exhaustedly studied for many years. The focuses are on the following: (1) intact rocks as a porous medium (Louis and Maini 1970), (2) a

single rock fracture as a tunnel in laboratory scale (Goodman 1970; Barton et al. 1985), and (3) fractured rock mass as an equivalent continuum porous medium in large scale (Witherspoon 2000). In this simulation, both the large-scale background and small-scale engineering are considered in determining permeabilities. Specific methods are described below.

Firstly, the rock mass permeability is treated as a constant value that reflects the hydrogeological background and is evaluated by means of some empirical models. An effective empirical model reflecting the relationships between hydraulic conductivity (K) and either the rock quality designation (RQD) or the RMR index was suggested by EI-Naqa (2001). With reference to the model, the RQD and the RMR were evaluated by means of field investigation and borehole data collection within the whole Zhaogezhuang coalmine area. Then, the relationships between the K and either the RQD or the RMR are established as an empirical model, from which the hydraulic conductivities of rock masses with different quality features can be obtained and serve as the background hydraulic conductivity (K_0). Taking the fault zone as an example, its hydraulic conductivity is 1.96×10^{-6} m/s.

Secondly, the permeability is also variable due to its coupling with the engineering stress under the influence of mining activities. For engineering scale problems, such as the excavation disturbed zone (EDZ) of a tunnel or a working face, the permeability may be changeable in response to the mining-induced stress field changes and can be coupled with the stress in a form of some mathematic expressions (Rutqvist and Stephansson 2003). Some empirical models have been used to match the permeability k versus the confining pressure σ_i and the fluid pressure p . The following exponential function (Louis et al. 1977) was adopted in one scenario in this study.

Table 3 A brief summary of the power law creep model for rocks in China coalmines

Model	Rock type	Testing method	Confining pressure σ_3 (Mpa)	Remarks
$\dot{\varepsilon} = 6.3 \times 10^{-4} \bar{\sigma}^{5.39} t^{-0.985}$	Fault mud	Triaxial	0.2	Modified from Zhou et al. (2000), samples from Zhaogezhuang coal mine
$\dot{\varepsilon} = 3.6 \times 10^{-8} \bar{\sigma}^{4.37} t^{-0.87}$	Milionite	Uniaxial	0	Modified from Zhou et al. (2000), samples from Zhaogezhuang coal mine
* $\varepsilon = 3 \times 10^{-5} q^{1.2} t^{0.25}$	Mudstone	In situ	(0, 2)	Cited from Chen et al. (2009b), samples from Xinji coal mine
** $\dot{\varepsilon} = 8.5 \times 10^{-7} \bar{\sigma}^{-0.11} t^{-0.11}$	Mudstone	In situ	(0, 2)	Modified from Chen et al. (2009b), samples from Xinji coal mine
^ $\varepsilon = 2.1 \times 10^{-5} \sigma^{1.25} t^{0.15}$	Mudstone	Triaxial	4	Cited from Chen et al. (2009a), samples from Xinji coal mine
^^ $\dot{\varepsilon} = 2.4 \times 10^{-7} \bar{\sigma}^{1.21} t^{-0.03}$	Mudstone	Triaxial	4	Modified from Chen et al. (2009a), samples from Xinji coal mine

* ε is strain, q is creep stress (in situ)
 ** $\dot{\varepsilon}$ is creep rate, $\bar{\sigma}$ is equivalent stress calculated by Eq. (2)
 ^ ε is strain, σ is creep stress (in-door)
 ^^ $\dot{\varepsilon}$ is creep rate, $\bar{\sigma}$ is equivalent stress calculated by Eq. (2)

$$k = k_0 \exp(-a_1(\sigma_t - p)) \quad (4)$$

where $a_1 = 0.221$ is a fitting parameter, modified from the results of the underground packing testing in Zhaogezhuang coalmine (Li and Gao 2003); and k_0 is a reference permeability ($\text{m}^2/(\text{Pa sec})$ in SI unit), which is the background permeability.

Numerical simulation

Hydromechanical coupling simulation

The hydromechanical coupling behavior can be described mathematically in a coupling relationship between a group of mechanics equations and fluid flow equations (Neuzil 2003; Rutqvist and Stephansson 2003). Three scenarios are considered separately as follows. (1) The rock materials are assumed to be the elastoplastic Mohr–Coulomb materials. The stresses are adjusted in accordance with the relative failure criterion or flow rules and coupled with water pressure by the elastoplastic strain–fluid coupling mechanism. In this simulation, the rock materials within the VIIIth fault zone are adopted as the Mohr–Coulomb materials. (2) The rock materials are assumed to be the creep materials. The stress adjustments are dependent upon the rheological constitutive model, e.g. the above-mentioned power law creep model, and coupled with water pressure by the creep–fluid coupling mechanism (Wu et al. 2011b; Zhu 2009). The rock materials of the fault gouge are adopted in the power law creep model. (3) The permeability is changeable with the mining-induced stress field, and it obeys the exponential function (Eq. 4) reflecting the stress–permeability coupling mechanism.

Mining process simulation

To study the water inrush development over the course of the mining activity, three mining phases are divided: (1) the first mining phase, simulating a period of excavating the 3132_1 working face out instantaneously and lasting 40 days, in application of the NULL elements on the group of “coal mining in the 1st phase” in FLAC^{3D} model (Fig. 3d); (2) the second mining phase, simulating a period of excavating the 3132_2 working face out and lasting 40 days, by use of the NULL elements in it, while filling analog materials as the imitation of 3132_1 working face collapses; and (3) the third mining phase, simulating a period of the 3132_3 excavation and the 3132_2 filling, as same as the operations occurring in 3132_2 and 3132_1 working faces in the last mining phase. The locations of coalmining working faces in each mining phase are shown in Fig. 3d.

Results

Evolution of water-recharge zones

Three scenarios corresponding to the three possible hydromechanical coupling behaviors of fluid–rock interactions within the fault zone were simulated: (1) an elastoplastic strain–fluid coupling mechanics of rock mass in the fault zone, (2) a creep–fluid coupling mechanics of rock materials in the fault gouge, and (3) a stress–permeability coupling mechanics of fractured rock mass in the fault zone influenced by excavation.

Simulation of scenario 1

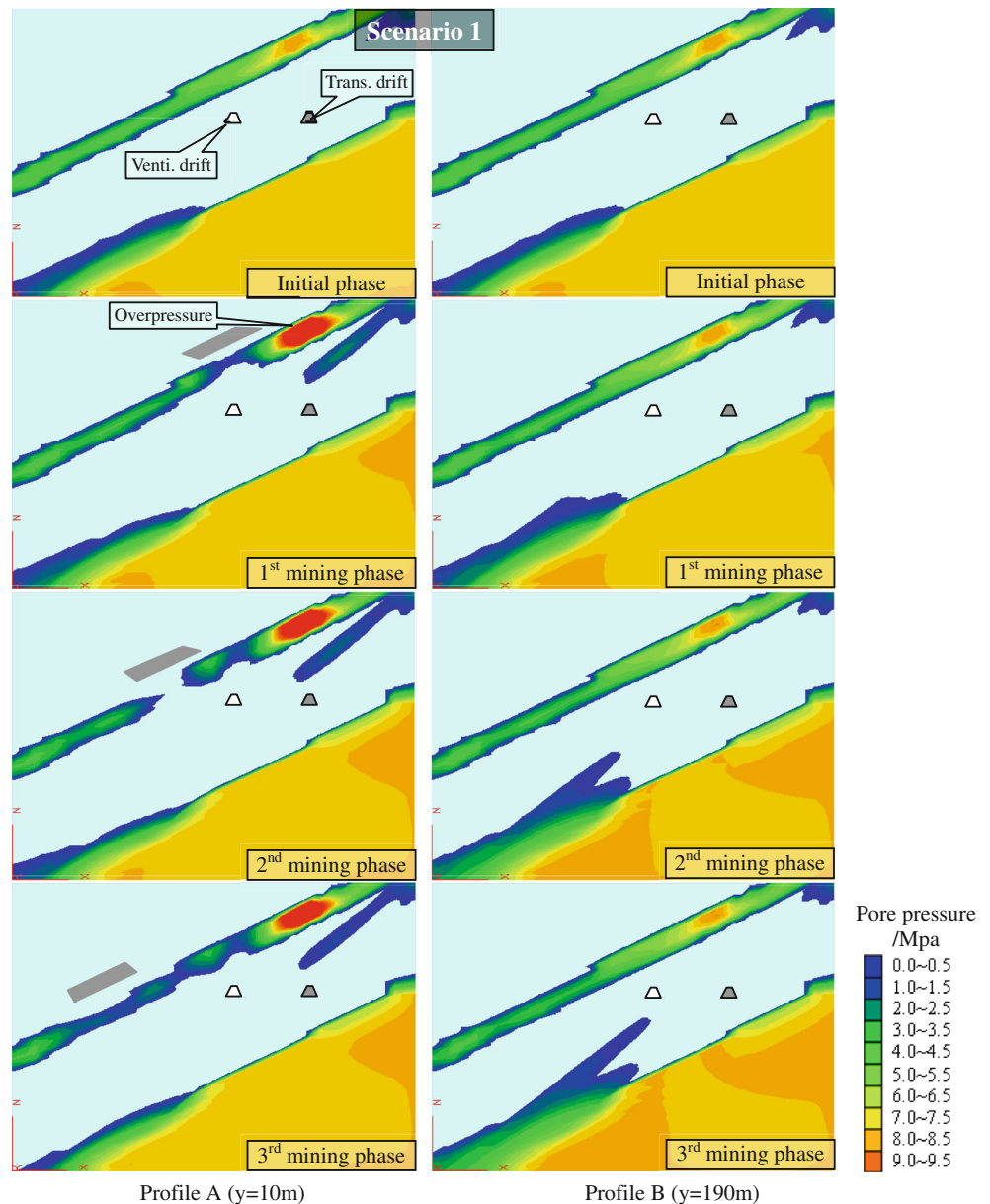
The development of water-recharge zones is depicted in profile A ($y = 10$ m) and profile B ($y = 190$ m), respectively (Fig. 4). In profile A, groundwater is flowing downward from the coal seam aquifer to the transportation drift along faults. The seepage flow field reaches the top-right of the transportation drift after the 3rd phase mining, about 20 m away, with a pore pressure of almost 2.0 Mpa. An upward seepage developed in the profile B from Ordovician limestone aquifer to the ventilation drift. The seepage front is about 20 m away from the bottom-left of the ventilation drift and has a pore pressure of around 0.5 Mpa.

In profile A, an abnormal overpressure zone within the coal seam aquifer is generated with a maximum of 9.0 Mpa. This reflects the fact that the overpressure is forming gradually as a result of the stress concentration at the end of a working face. The downward seepage flow is mainly driven by the excessive pore pressure, and hence a high risk of water inrush may exist in the transportation drift. This may also explain why there is more groundwater flooding into the 13th level transportation drift than the ventilation drift in the study site.

Simulation of scenario 2

When the power law creep model (Eq. 3) was utilized in the fault gouge, the coupling process can be achieved in FLAC^{3D}. In assumption of the creep–fluid coupling mechanics, the development of a water-recharge zone is very different with it in the previous scenario (Fig. 5). From the initial phase of this scenario, the water-recharge zone exhibits a form of downward seepage flow along the fault. It means that the water-recharge zone has formed before mining. As the mining progresses forward, the seepage flow seems not to have a trend of slight devolution in profile A ($y = 10$ m); however, a downward seepage flow in profile B ($y = 190$ m) develops continuously until

Fig. 4 Results of scenario 1 in which the elastoplastic strain model was assigned to the fault zone. *Left* Evolution of the water-recharge zone and downward seepage flow from the coal measure aquifer in profile A ($y = 10\text{ m}$). *Right* Evolution of the water-recharge zone and upward seepage from the Ordovician limestone aquifer in profile B ($y = 190\text{ m}$)



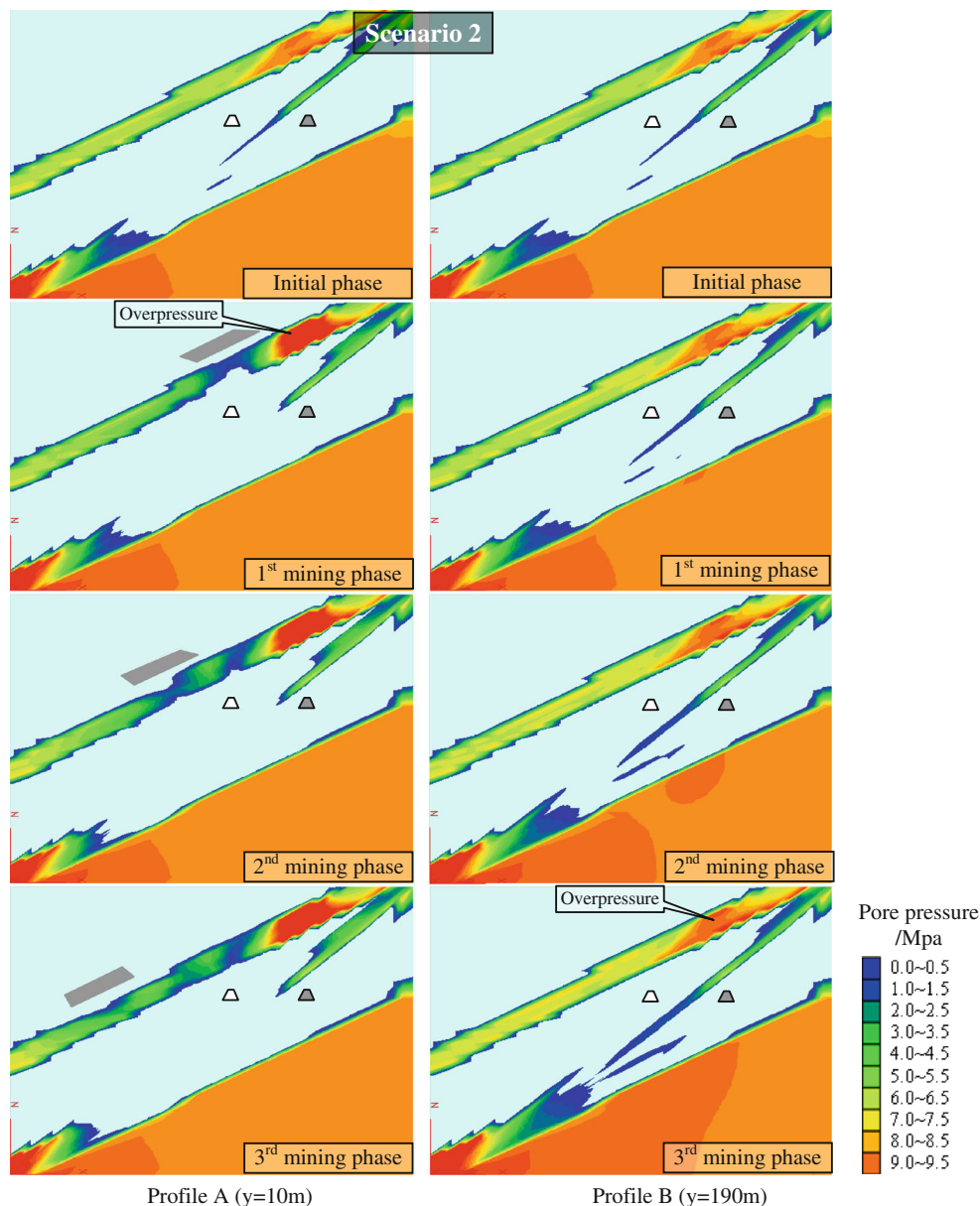
its leading front meets with the upward seepage flow from the Ordovician limestone aquifer.

An abnormal overpressure zone is also observed in the coal measure aquifer, with a highest value of 9.5 Mpa in profile A after the first mining phase. Pore pressure in the water-recharge zone is able to reach 5.0 Mpa. Therefore, there exist more risks of water inrushes in this scenario than the previous one. Once favorable or advantageous rock fractures are present under the influence of mining activity, the long-term accumulation of overpressure will be released in the form of an influx into open spaces, such as drifts and working faces, consequently leading to the occurrence of water inrushes.

Simulation of scenario 3

On the engineering scale, rock permeability variations induced by mining activities may be worth considering around the EDZ. The permeability is free to change governed by Eq. (4) in this scenario, although the rock materials in the fault gouge are still represented using the power law creep model. The simulation results are shown in Fig. 6. It can be found that the pore pressure field is almost the same as the modeling results in scenario 2. This implies that the permeability variations induced by mining activities at such a depth are not enough to significantly affect the pore pressure distribution and the evolution of water-recharge zones.

Fig. 5 Results of scenario 2 in which the power law model was assigned to the fault zone. It shows significant differences with scenario 1. *Left* Evolution of the water-recharge zone and downward seepage flow from the coal measure aquifer in profile A ($y = 10$ m). *Right* Evolution of the water-recharge zone and upward seepage from the Ordovician limestone aquifer in profile B ($y = 190$ m)



Comparison of simulated results with in situ monitoring results

The ‘history’ command in FLAC^{3D} provides a convenient method to monitor the simulated results, such as stress, strain, displacement, temperature, and pore pressure (Itasca Consulting Group 1997). A number of monitoring points can be set up to record pore pressure changes with time. Two representative monitoring points (Hist. A and Hist. B) have been labeled in the model profiles A and B (Fig. 6), respectively, for the purpose of observing the pore pressure changes in the fault zone, and comparing simulated results with the in situ monitoring results data of water pressure.

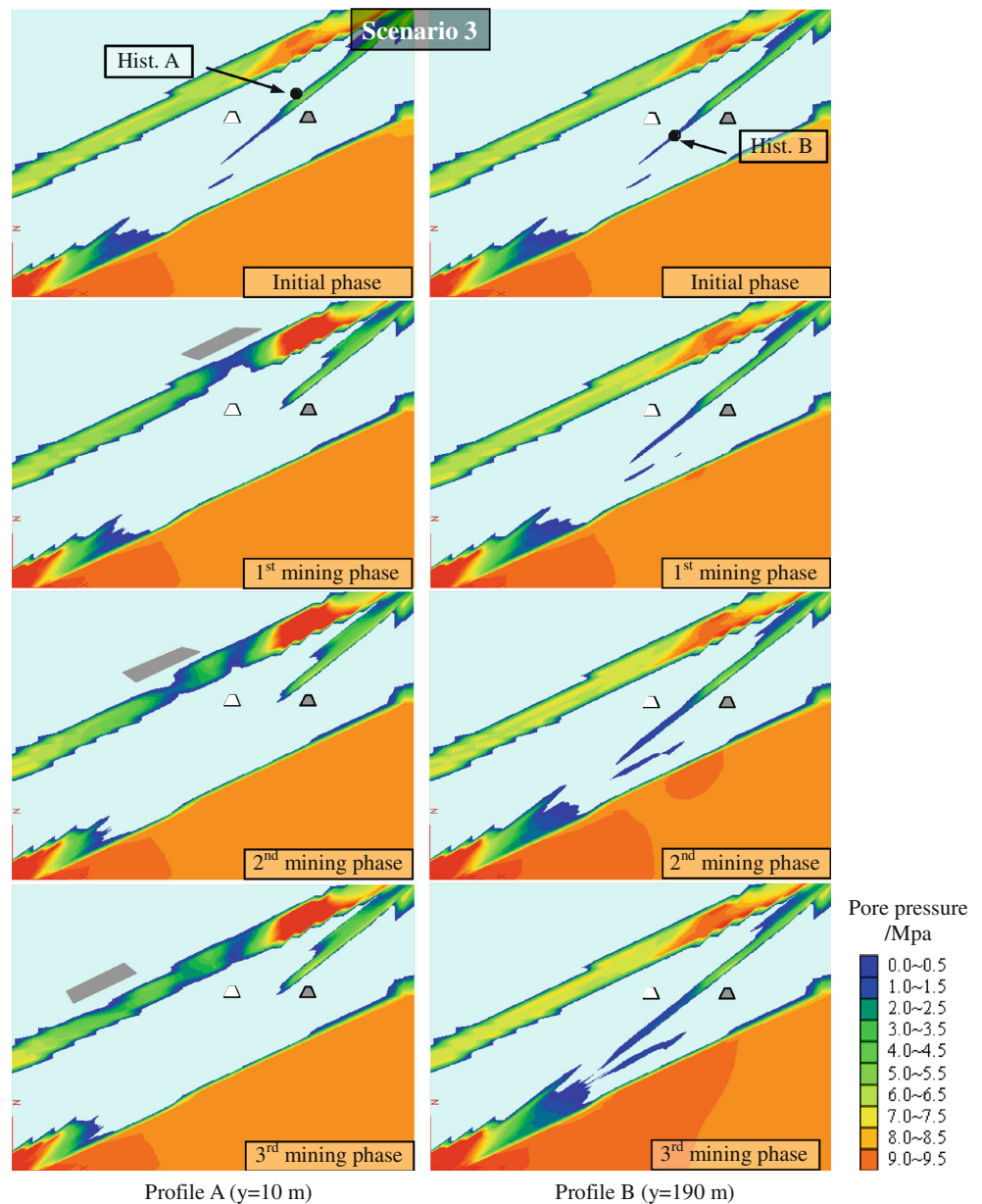
Fig. 7 shows the simulated pore pressure changes with time under two assumptions: (1) the creep-fluid coupling

mechanism (dash line), and (2) the elastoplastic strain-fluid coupling mechanism (solid line). The starting and the ending times of the three simulated mining phases are also indicated by the curve of the max unbalanced force (red solid line), a mechanical indicator of the total equilibrium state of a system during a whole simulation period.

Elastoplastic strain-fluid coupling simulation

The solid black lines in Fig. 7 show that the pore pressure curves have a fluctuation of up and down in a relatively short period. The simulated peak pore pressures reach about 1.8 and 5.5 Mpa in the 1st and 2nd mining phase, respectively. However, the peak pressure can be found over

Fig. 6 Results of scenario 3 in which the power law model with a variable permeability was assigned to the fault zone. *Left* Evolution of the water-recharge zone and downward seepage flow from the coal measure aquifer in profile A ($y = 10$ m). *Right* Evolution of the water-recharge zone and upward seepage from the Ordovician limestone aquifer in profile B ($y = 190$ m). The results are very similar with the modeling of scenario 2 in Fig. 5. Notice that the positions of Hist.A and Hist.B in model are shown in the initial phase. The pore pressure changes with time on these spots were recorded during modeling



a relatively short period of time, unlike in the creep-fluid coupling simulation the peaks last for a long time.

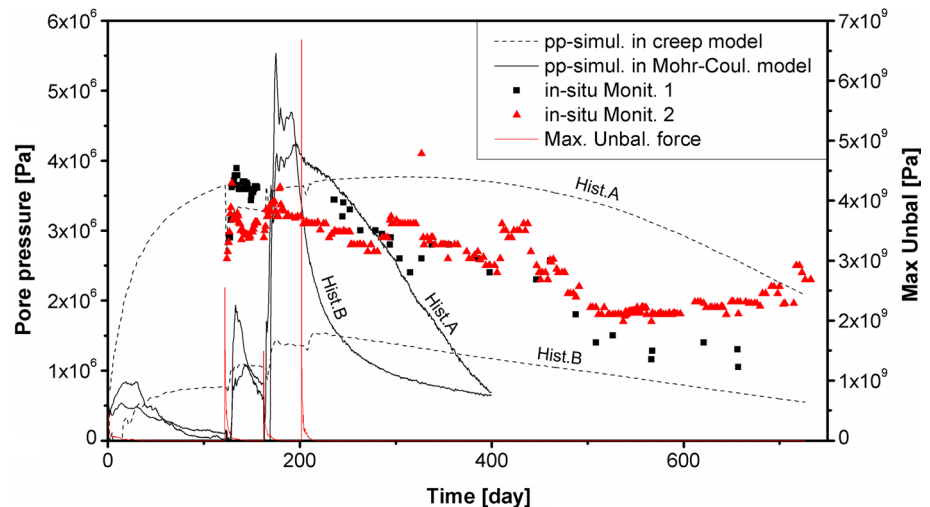
This is mainly because the elastoplastic constitutive models can only reflect the short-term mechanical behaviors of rock materials and cannot depict the mechanical behaviors of the long-term trends.

Creep-fluid coupling simulation

The pore pressure curves in dash lines, labeled with Hist. A and Hist. B, respectively, present a slow variation over the whole simulation period. Note that the pore pressure curves are disturbed at the starting time point of every mining phase, and these disturbances are obviously

discernible in the form of step-style variations. The maximum reaches about 3.8 Mpa and lasts for a while in Hist. A, and about 1.6 Mpa with gently depletion in Hist. B, respectively. Also, the pore pressures in this scenario seem to follow a preset path; and they tend to gradually return to the original track after being disturbed by mining activities, as if they are of self-healing and have memory capacity. This kind of self-healing phenomenon often occurs in clay-stone, such as Boom clay, whose self-healing capacity of argillaceous rocks has been researched by Van Geet et al. (2008) in laboratory. This implies that the fault gouge in our study area may also have this kind of property and capacity from a hydraulic point of view.

Fig. 7 Pore pressure (pp) evolution with time of scenario 1 (solid line) and scenario 2 (dash line). The in situ monitored water pressure values from monitoring points 1 (black scatter) and 2 (red scatter) are also plotted as a reference. Meanwhile, the max unbalanced force (red solid line) is shown as a benchmark of the beginning and ending time of three simulated mining phases



Stress-permeability coupling simulation

The simulated pore pressure curves corresponding to the stress-permeability coupling mechanism are shown in (Fig. 1 ESM only). Unlike the first two simulation results, each curve now has no obvious depletion segments, and the changes in pore pressure are within a narrow range from 3.78 up to 3.85 Mpa in Hist. A and from 1.63 down to 1.56 Mpa in Hist. B, in the later period of simulation. This may be related to the division of the EDZ range. A reasonable division for EDZ will be helpful to get better simulation results.

Comparison between simulation results and in situ observations

For the sake of comparison, the simulated curves and in situ monitoring data are plotted together in Fig. 7. The in situ water pressures exhibit a long-term trend of a slow variation rate on the whole, but locally have a behavior characterized by a short-term up and down fluctuation. The in situ data are generally in good agreement with the simulation results of the creep-fluid coupling model, and also show similar short-term fluctuations with the modeling results of the elastoplastic strain-fluid coupling model. A possible explanation for this is that the rock masses within the fault zones are characterized hydraulically by a long-term trend in the creep-fluid coupling simulation and by a short-term effect in the elastoplastic strain-fluid coupling simulation.

It has been manifested by field observations (Li and Zhou 2006) that the pore pressure changes are almost simultaneous with the flow rate changes. Some analytical solutions also show the synchronization of the changes of hydraulic head and flow rate, such as Cornaton and Perrochet (2002), in which some simulation results demon-

strate this synchronization although their paper does not aim to address this issue. All the things mean that the water discharge or flow rate is related with the pore pressure directly. In accordance with the regulations of coalmine water prevention and control in China (2009), when the flow rate is up to 10–30 m³/min, it is termed as a water inrush, which can be detected through the in situ monitoring of water pressure (also pore pressure) changes.

Obviously, for the lagging water inrush, the water pressure is a vital indicator for monitoring and forecasting. From the perspective of the two kinds of numerical simulation results, the pore pressure simulated by the elastoplastic strain-fluid coupling is the key to trigger the risk of a water inrush when it exceeds the one simulated by the creep-fluid coupling.

Theoretical discussion on simulation results and its physical meaning

The two simulated pore pressures seem to be explained by the dual-porosity model (DPM). The basic concept of DPM is that the fractured rock consists of two overlapping continua in interaction: a matrix continuum of low-permeability and primary porosity and a fracture continuum of high-permeability and secondary porosity; and the two distinct values of the piezometric head or pore pressure are attributed to the same representative elementary volume (REV) of the fractured rock, taking into account the presence of different groups of pores (families of fractures, porous matrix). In the traditional form, this approach takes into account that the highly permeable fractures respond faster than the porous matrix to external disturbances, e.g., pumping wells, rainfall infiltration, river flooding. In reality, the two pore pressures are difficult to be measured. In most cases, the measured values represent their mixed

piezometric head. Therefore, the numerical simulation or the analytical solution to a specific problem of DPM is an inevitable approach.

For the mining disturbance, the first to generate a response should be the pore pressure of the fractures continuum. The pore pressure changes occurred in the fractures continuum have the typical hydraulic behaviors of short-term effects and could be simulated by the elastoplastic strain-fluid coupling in assumption that the fractured rock mass are as the elastoplastic Mohr–Coulomb materials. In a practical situation, it is presented as a phenomenon of the rapidly and frequently fluctuation of the water pressure or the flow rate, and is disadvantageous to water inrush prevention. By contrast, the pore pressure changes occurred in the porous matrix always have the hydraulic behaviors of slow and stable long-term effects and could be simulated by the creep-fluid coupling in assumption that the rock materials within the fault zone (including fault gouge) are as the creep materials. In realistic situation, it is shown as a process of the slow water

pressure releasing, and is advantageous to water inrush prevention. When the pore pressure of the fractures continuum exceeds that of the porous matrix, it means that the water pressure releasing or inflow into drafts will not be in the slow or the controllable manner, but in the sudden or the water inrush way.

This simulation method is different from the traditional method, such as the water inrush coefficient method, in which the impact of the measured pressure in the underlying aquifer will be more considered on the risk of water inrush. However, some practical problems are hard to be explained based on the traditional method. For example, some water inrush incidents happened in places always thought to be safe using water inrush coefficient method, e.g., the 1972 water inrush at the 9th level of no. 1 crosscut, at the depth of approximately -730 m, in the same coalmine (Wu et al. 2002; Zhu 2009), while water inrushes did not take place in places with more heavy water pressure, e.g., the 13th level of no. 1 crosscut as described in this paper. This numerical simulation approach based on the

Fig. 8 Diagram to show how to determine the ‘time window’ in which the risk of lagging water inrush is high in every mining phase based on pore pressure evolution curves at **a** Hist. A and **b** Hist. B. Notice that the beginning time of the 1st mining phase has been considered as the starting point of the lag time

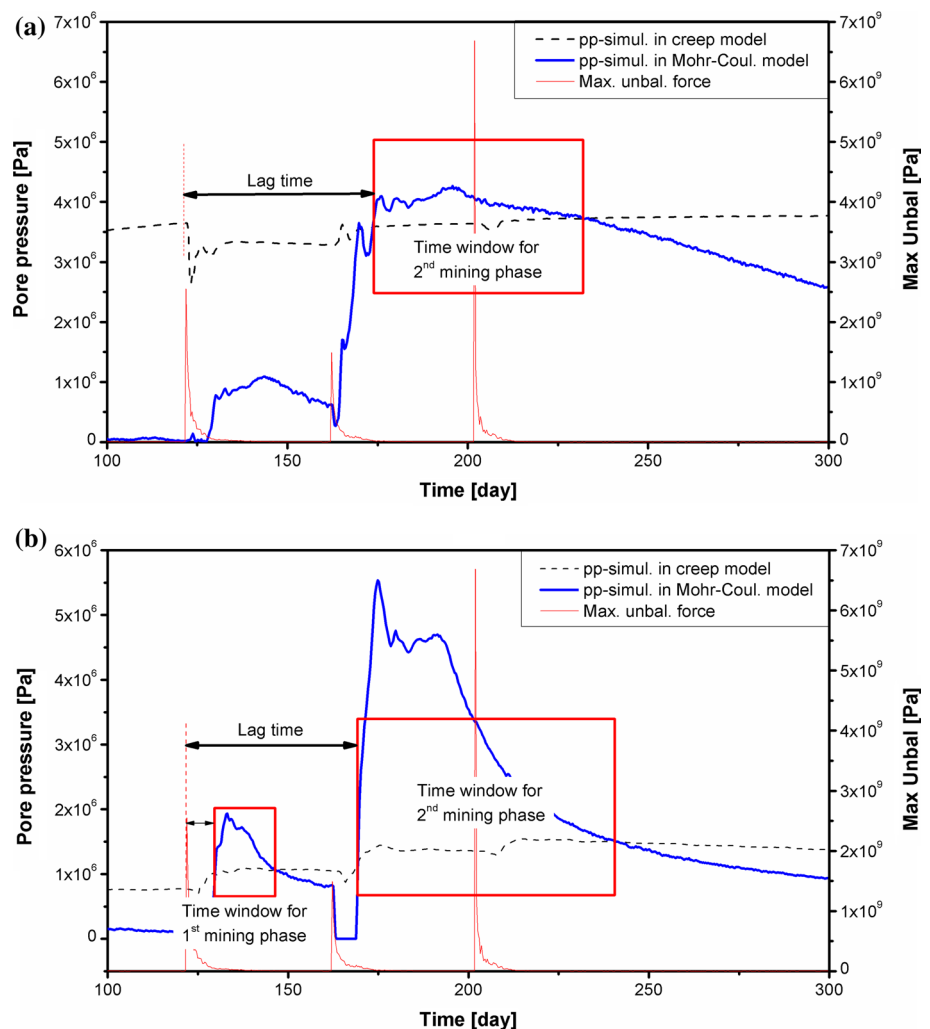


Table 4 Statistical parameters of the ‘time window’ for the risk of water inrush occurrence

Position	1 st mining phase				2 nd mining phase				3 rd mining phase					
	Lag time/day		Time window		Lag time/day		Time window		Lag time/day		Time window			
			Open	Close			Open	Close			Open	Close		
	P.P./Mpa	Time/day	P.P./Mpa	Time/day	P.P./Mpa	Time/day	P.P./Mpa	Time/day	P.P./Mpa	Time/day	P.P./Mpa	Time/day		
Hist.A	–	–	–	–	–	52	3.59	174	3.73	234	–	–	–	–
Hist.B	7	1.01	129	1.07	147	47	1.07	169	1.50	240	–	–	–	–

DPM makes it possible to forecast the water inrush by simulating the process of the seepages along the fault zone.

Feasibility of a prediction method for lagging water inrush

In this section, a potential prediction method for lagging water inrush is discussed based on the simulation results. A concept of ‘time window’ is proposed in order to better predict the lagging water inrush. Based on the simulated results shown in Fig. 8, the point in time when the pore pressure of the short-term effects exceeds the one of the long-term trends can be determined as the dangerous time point of a water inrush. In other words, the ‘time window’ opening for the risk of a water inrush can be determined at this time point. Similarly, the ‘time window’ closing can be defined on the basis of the reverse rules. The width of ‘time window’ from the opening to the closing can be defined as the critical phase of a water inrush occurrence. Figure 8 shows how to determine the ‘time window’ by means of the two pore pressures at the sites of Hist. A (Fig. 8a) and Hist. B (Fig. 8b), respectively, which are the locations within the coverage of the water-recharge zone. The ‘time window’ concept means that the long-term pore pressure is considered as a benchmark of critical value in the risk of water inrush. The benchmark also could be a specified upper-limit value as matter of experience, e.g., a statistical water pressure or corresponding inflow flux enough safe to avoid the risk of water inrush. In this case, the ‘time window’ is still applicable.

Figure 8 also illustrates a method of determining the ‘time window’ and dividing the different phases. For the purpose of observation, the time span is limited from 100 to 300 days so that the readers can zoom to see more details in an enlarged map. As an aid, the starting time of the 1st mining phase reflected by the pulse-wave curve of max unbalanced force serves as the starting point to count the lag time; and then, the ‘time window’ opening or closing is dependent upon the point of time when the pore pressure of the short-term effects are above or below the one of the long-term trends in each mining phase,

respectively. The statistical parameters of the ‘time window’ for lagging water inrush are shown in Table 4.

From Table 4, it can be seen that the lagging water inrushes most likely occur in the first two mining phases. In particular, the 2nd mining phase represents the most dangerous phase, with 60 and 71 days of the critical phase, and 52 and 47 days of the lag time in Hist. A and Hist. B, respectively. The 3rd mining phase is likely a safe period.

Generally, rheological deformations are thought to be a slow process; therefore, there is plenty of time for the pore pressure to release slowly and the excessive pore pressure will not be easy to form during the creep-fluid coupling process. Whereas, most of elastoplastic deformations are considered to occur in a short period of time, even if the time adjusting the secondary stress field is took into account. The excessive pore pressure caused by mining can be quickly gathered within a short period of time and move along with the fractured fault zones in the form of a seepage flow. When there are some opening spaces, such as drifts, working faces and so on, on the path of the seepage flow, the excessive pore pressure can be released quickly by an influx of water flow. That is the reason why a water inrush occurs easily over the course of mining and usually there is a lag time from the excessive pore pressure gathering to the water inrush occurring.

Conclusions

A process-based numerical model with the hydromechanical coupling simulation for mining excavation has been described. The underlying concept for this study is to utilize two kinds of coupling, i.e., the elastoplastic strain-fluid coupling and the creep-fluid coupling, for simulating the non-linear water inrush process. The simulated evolution of water-recharge zones has revealed a possible development process of the small-scale lagging water inrush, involving the flow routing, scaling, recharging and changing, which occurred in the 13th level of no. 1 crosscut, about – 1,100 m depth, in Zhaogezhuang coalmine.

The simulation results corresponding to different coupling mechanisms exhibit prominent differences in pore-fluid pressure distribution. The creep-fluid coupling simulation reflects the rock mass of hydraulic behaviors of long-term trends, and the elastoplastic strain-fluid coupling simulation demonstrates its short-term effects. The overall trends and the short-term effects displayed in the field observation are explained by the simulation results. It can be drawn that the rock mass hydraulic behaviors are characterized by a combination of the long-term trends and the short-term effects. The double-porosity characteristics of the rock formation may play an important role in controlling the lag-time water intrusions.

Also, a practical method called ‘time window’ for forecasting the risk of a water intrusion has been developed in this study. Some of the key parameters of time window, such as the lag time, opening, critical phase and closing, can be determined through an overlay map of the two simulation curves, on a basis of the assumption that the long-term hydraulic trends depend on the creep-fluid coupling and the short-term hydraulic effects rely on the elastoplastic strain-fluid coupling.

It is always a confusing problem in rock parameters determination due to an insufficient understanding of the differences in rock mass properties between a sample scale and an engineering scale. Therefore, a great deal of efforts has been put into the aspect of collecting and analyzing previous experiments data of both in door or in situ. The rheological parameters of the power law creep model have a great difference from previous works. In our modeling, A , n and m are determined to be $1.01e-7$, 3.0 and 0.1, respectively, mostly based on the rheological tests data and partially referred to early experience. With these parameters, our numerical simulation has reached the basic objective, that is, the interpretation of general trends, in spite of the lack of re-fining parameters.

The simulation results based on the stress-permeability coupling model are similar to those based on the creep-fluid coupling model in the evolution of the water-recharge zones and seepage flow. However, the curves of pore pressure versus time have some differences, which seem not to be very consistent with the in situ data. A possible solution is that the EDZ should be postulated or preset, combining with an automatic adjustment by means of controlling the independent variables, e.g. the strain, the stress and the pore pressure, within the limited range of EDZ. The stress-permeability model considering the permeability interaction with stress is of more reasonable.

Acknowledgments This work was supported by a Kailuan Group Corporation Grant (No: KL tech. [2011]181). The research was also partially supported by the Program to Sponsor Teams for Innovation in the Construction of Talent Highlands in Guangxi Institutions of Higher Learning. The constructive comments from the editor and

anonymous reviewers are greatly appreciated. Supported by Kailuan Group Corporation and Key Laboratory of Geological Engineering Centre of Guangxi

References

- Barton NR, Lien R, Lunde J (1977) Estimation of support requirements for underground excavations. In: 16th US Symposium Rock Mech, pp 164–177
- Barton NR, Bandis S, Bakhtar K (1985) Strength, deformation and conductivity coupling of rock joints. *Int J Rock Mech Min Sci Geomech Abstr* 22:121–140
- Bäckblom G, Martin CD (1999) Recent experiments in hard rock to study the excavation response: implication of the performance of a nuclear waste geological repository. *Tunn Undergr Space Technol* 14:377–394
- Bieniawski ZT (1984) Rock mechanics design in mining and tunneling. A.A. Balkema, Rotterdam, p 272
- Börgesson L, Pusch R, Fedriksson A, Hökmark H, Karnland O, Sandè NS (1992) Final report of the zones disturbed by blasting and stress release. Swedish Nuclear Fuel and Waste Management Co (SKB), Stockholm. Stripa Proj Tech Rep 92–08
- Cai M (2011) Rock mass characterization and rock property variability considerations for tunnel and cavern design. *Rock Mech Rock Eng* 44:379–399
- Caillabet Y, Fabrie P, Landerau P, Noetinger B, Quintard M (2000) Implementation of a finite-volume method for the determination of effective parameters in fissured porous media. *Numer Methods Partial Differ Equ* 16:237–263
- Cao YX, Qi CQ (2004) A feasibility study of changeover from fragmental water supply to round-the-clock water supply, a case study of Zhaogezhuang mine. *Coal Geol China* 16(Sup):40–42
- Chen WZ, Tan XJ, Lu SP, Yang JP et al (2009a) Research on large-scale triaxial compressive rheological test of soft rock in depth and its constitutive model. *China J Rock Mech Eng* 28(6): 1735–1744
- Chen WZ, Yu HD, Wang XQ, Jia SP et al (2009b) Development of a double linkage triaxial testing machine for hydro-mechanical coupling in soft rock. *China J Rock Mech Eng* 28(11): 2176–2183
- Coalfield Geological Central Bureau of China (2000) Coalfield hydrogeology of China. Coal Industry Publishing House of China, Beijing, pp 15–59
- Cornaton F, Perrochet P (2002) Analytical 1D dual-porosity equivalent solutions to 3D discrete single-continuum models. Application to karstic spring hydrograph modeling. *J Hydrol* 262:165–176
- EI-Naqa A (2001) The hydraulic conductivity of the fractures intersecting Cambrian sandstone rock masses, central Jordan. *Environ Geol* 40:973–982
- Emsley S, Olsson O, Stenberg L, Alheid H-J, Fall S (1997) ZEDEx—a study of damage and disturbance from tunnel excavation by blasting and tunnel boring. Swedish Nuclear Fuel Waste Management Co. (SKB), Stockholm. Tech Report 97–30
- Gerya TV, Stckhert B, Perchuk AL (2002) Exhumation of high-pressure metamorphic rocks in a subduction channel: a numerical simulation. *Tectonics* 21(6):1056–1081
- Goodman RE (1970) Deformability of joints. In: Proceedings symposium determination of the in situ modulus of deformation of rock, 2–7 February, Denver, Colorado. ASTM Spec Tech Publ 477, pp 174–196
- Goodman R, Moye D, Schalkwyk A, Javendel I (1965) Ground-water inflow during tunnel driving. *Eng Geol Bull IAEG* 2(1):39–56

- Granet S, Fabrie P, Lemonnier P, Quintard M (2001) A two-phase flow simulation of a fractured reservoir using a new fissure element method. *J Petrol Sci Eng* 32(1):35–52
- Gray M (1993) OECD/NEA international Stripa project 1980–1992. Overview volume III, engineered barriers. SKB, Stockholm
- Heuer R (1995) Estimating rock tunnel water inflow. In: Proceedings of rapid excavation and tunnelling conference, 1995, pp 41–60
- Hoek E, Brown ET (1997) Practical estimates of rock mass strength. *Int J Rock Mech Min Sci* 40:701–710
- Itasca Consulting Group (1997) Flac3D, Fast lagrangian analysis of continua in 3 dimensions, user's manual, 2nd edn. Itasca Consulting Group Inc, Minneapolis
- Justo JL, Justo E, Azañón JM, Durand P et al (2010) The use of rock mass classification systems to estimate the modulus and strength of jointed rock. *Rock Mech Rock Eng* 43:287–304
- Li XG, Gao YF (2003) Influence of mining on floor infiltration coefficients. *Chin J Rock Mech Eng* 22(7):1078–1082
- Li GY, Zhou WF (2006) Impact of karst water on coal mining in North China. *Environ Geol* 49:449–457
- Long JCS, Remer JS, Wilson CR, Witherspoon PA (1982) Porous media equivalents for networks of discontinuous fractures. *Water Resour Res* 18(3):645–658
- Louis C, Maini Y (1970) Determination of in situ hydraulic parameters in jointed rock. In: Proceedings 2nd international congress rock mechanics, 21–26 September 1970, Belgrade. *Inst Dev Water Resour, Belgrade, vol I*, pp 235–245
- Louis C, Dessenne J-L, Feuga B (1977) Interaction between water flow phenomena and the mechanical behavior of soil or rock masses. In: Gudehus G (ed) *Finite elements in geomechanics*. Wiley, New York, pp 479–511
- McFeat-Smith I, Turner VD, Bracegirdle DR (1985) Tunnelling conditions in Hong Kong. *Hong Kong Eng* 13(6):13–25
- McFeat-Smith I, MacKean R, Waldmo O (1998) Water inflows in bored rock tunnels in Hong Kong: prediction, construction issues and control measures. In: ICE conference on urban ground engineering, Hong Kong
- Neuzil CE (2003) Hydromechanical coupling in geologic processes. *Hydrogeol J* 11:41–83
- Norton FH (1929) *Creep of steel at high temperatures*. McGraw-Hill Book Company, New York
- Olsson O (1992) Site characterization and validation—final report: Stripa Project. Swedish Nuclear Fuel Waste Management Co, Stockholm. Rep TR 92–22
- Perello P (2011) Estimate of the reliability in geological forecasts for tunnels: toward a structured approach. *Rock Mech Rock Eng* 44:671–694
- Rutqvist J, Stephansson O (2003) The role of hydromechanical coupling in fractured rock engineering. *Hydrogeol J* 11:7–40
- Sitharam TG, Sridevi J, Shimizu N (2001) Practical equivalent continuum characterization of jointed rock masses. *Int J Rock Mech Min Sci* 38(3):437–448
- Sugihara K, Matsu H, Sato T (1999) In situ experiments on rock stress conditions and excavation disturbance in JNC's geoscientific research program in Japan. In: Saeb S, Francke C (eds) *Proceedings international Worksheet Rock Mechanics of Nuclear Waste Repositories*, 5–6 June. Veil, Colorado, pp 159–183
- Sun J (2007) Rock rheological mechanics and its advance in engineering applications. *China J Rock Mech & Eng* 26(6):1081–1106
- Tao B, Wu FQ, Guo GM et al (2005) Flexibility of visco-elastoplastic model to rheological characteristics of rock and solution of rheological parameter. *China J Rock Mech & Eng* 24(17):3165–3172
- Van Geet M, Bastiaens W, Ortiz L (2008) Self-sealing capacity of argillaceous rocks: review of laboratory results obtained from the SELFRAC project. *Phys Chem Earth* 33:s396–s406
- Wang SZ, Hou WY, Tang HM, Xiao ZR et al (1977) Report of extending geological survey within Linxi-Zhaogezhuang coalmine. Kailuan group corporation, Tangshan, pp 10–18
- Witherspoon PA (2000) The Stripa project. *Int J Rock Mech Mining Sci* 37:385–396
- Wu YS, Chen YW (1992) Rheologic test and simulation analysis of large scale in situ triaxial compression on defective strata behaviour. *Rock Soil Mech* 13(1):21–29
- Wu Q, Liu JT, Zhong YP, Yin ZR et al (2002) The numeric simulations of water-bursting time-effect for faults in Zhaogezhuang coalmine, Kailuan, China. *J China Coal Soc* 27(5):511–516
- Wu Q, Wang MY, Wu X (2004) Investigations of groundwater bursting into coalmine seam floors from fault zones. *Int J Rock Mech Min Sci* 41(4):557–571
- Wu Q, Liu YZ, Liu DH, Zhou WF (2011a) Prediction of floor water inrush: the application of GIS-Based AHP vulnerable index method to Donghuantuo coalmine, China. *Rock Mech Rock Eng* 44:591–600
- Wu Q, Zhu B, Liu SQ (2011b) Flow-solid coupling simulation method analysis and time identification of lagging water inrush near mine fault belt. *Chin J Rock Mech Eng* 30(1):93–104
- Zhou RG, Cheng BF, Gao YS et al (1998) Relationship between creep behavior of fault gouge and its water contents. *China J Eng Geol* 6(3):217–222
- Zhou RG, Cheng BF, Ye GJ et al (2000) Time effect of water inrush in fault rupture zone. *China J Eng Geol* 8(4):411–415
- Zhu B (2009) Research on fluid-mechanical interaction simulation and application on lagging water inrush near fault zone. Working report of post-doctoral fellow. China university of mining and technology, Beijing, pp 1–10